G^1 RANGE RESTRICTED DATA INTERPOLATION USING BÉZIER TRIANGULAR PATCH

SI PING

UNIVERSITI SAINS MALAYSIA

2015

G^1 RANGE RESTRICTED DATA INTERPOLATION USING BÉZIER TRIANGULAR PATCH

by

SI PING

Thesis submitted in fulfillment of the requirements of the Degree of Master of Science

February 2015

ACKNOWLEDGEMENT

I would like to take this opportunity to express my appreciation to my supervisor Dr. Kong Voon Pang for his invaluable support, guidance, supervision in my research and the preparation of this thesis.

My sincere appreciation to the Universiti Sains Malaysia especially the Dean of the School of Mathematical Sciences allowing me to pursue my higher degree here. I would like to acknowledge the financial support of the Fundamental Research Grant Scheme of Malaysia.

Besides this, I would like to thank my lover, parents and family members who were always there for me. With their support, I've gained courage to strive on especially when I was having difficulty in completing my dissertation.

Last but not least, I would like to express my gratitude to all my friends for giving me ideas and assistance in times of dire needs throughout my postgraduate program.

Thank you.

TABLE OF CONTENTS

ACKNOWLEDGEMENT ii

TABLE OF CONTENTS iii

LIST OF TABLES vi

LIST OF FIGURES vii

ABSTRAK xi

ABSTRACT xii

CHAPTER 1 INTRODUCTION 1

CHAPTER 2 TRIANGULAR BERNSTEIN-BÉZIER PATCH 8

2.0 Introduction 8

2.1 Bernstein Polynomials 9

2.2 Bézier Curve 11

2.3 Degree Elevation of Bézier Curve 11

2.4 Triangular Bézier Patch 12

2.5 Directional Derivatives of Bézier Patch 14

2.6 Normal Estimation 17

CHAPTER 3 G^1 CONTINUOUS JOIN OF QUARTIC BÉZIER TRIANGULAR PATCHES 20

3.1 C^1 Parametric Continuity Conditions 20

	3.2	G^1 Geometric Continuity Conditions	22
	3.3	C^1 Continuity as a Special Case of G^1 Continuity	33
	3.4	Intermediate Points $\boldsymbol{A}_3$, $\boldsymbol{B}_1$, $\bar{\boldsymbol{A}}_2$ and $\bar{\boldsymbol{B}}_2$	34
	3.5	Coefficients α, β and γ in G^1 Continuity Condition	36
		3.5.1 Repositioning Point $\boldsymbol{C}$	40
		3.5.2 Repositioning Points $\boldsymbol{A}$ and $\boldsymbol{D}$	41
CHAPTER 4	**SUFFICIENT NON-NEGATIVITY CONDITION FOR QURATIC BÉZIER TRIANGULAR PATCH**		43
	4.0	Introduction	43
	4.1	Signed Distance	43
	4.2	Sufficient Non-negativity Condition	44
CHAPTER 5	**G^1 RANGE RESTRICTED SCATTERED DATA INTERPOLATION**		52
	5.0	Introduction	52
	5.1	Triangular Surface Patch and Notation	55
	5.2	Patch's Boundaries	57
		5.2.1 Quartic Boundary Curves	61
		5.2.2 Constrained Boundary curves	61
	5.3	Inner Bézier Points Adjacent to a Boundary	68
		5.3.1 G^1 Patch	69
		5.3.2 G^1 Constrained Patch	74
	5.4	Convex Combination Bézier Patch	78

CHAPTER 6 GRAPHICAL RESULTS AND CONCLUSION 79

6.1 Graphical Results 79

6.2 Conclusion 94

6.3 Future Work 96

REFERENCES 97

APPENDIX 99

LIST OF TABLES

Table 6.1	Data of Example 1	80
Table 6.2	Data of Example 2	82
Table 6.3	Scattered data of Example 3	84
Table 6.4	Scattered data of Example 4	87
Table 6.5	Scattered data of Example 5	90
Table 6.6	Example 6: Rainfall Data of Penang island on 27/12/2014	93

LIST OF FIGURES

Figure 2.1	Triangle T with vertices $\boldsymbol{V}_1$, $\boldsymbol{V}_2$, $\boldsymbol{V}_3$	10
Figure 2.2	Directions at a boundary point e_1	16
Figure 2.3	Vertex $\boldsymbol{O}$ and surrounding triangles	18
Figure 2.4	A boundary vertex $\boldsymbol{O}$	19
Figure 3.1	Two adjoining domain triangles	20
Figure 3.2	Control points of two adjacent quartic Bézier patches	21
Figure 3.3	The shared pairs of triangles formed by control points of Bézier patches and the domain triangles	22
Figure 3.4	Three directions on domain triangles	23
Figure 3.5	A 'ridge' along the common boundary between two patches if $\alpha\beta < 0$	25
Figure 3.6	A pair of tangent triangles at vertex $\boldsymbol{V}_1$	28
Figure 3.7	A pair of tangent triangles at vertex $\boldsymbol{V}_2$	29
Figure 3.8	Geometric interpolation of (3.15)	31
Figure 3.9	Geometric interpolation of (3.16)	32
Figure 3.10	Intermediate points A_k, $\boldsymbol{B}_k$, $\bar{\boldsymbol{A}}_k$, $\bar{\boldsymbol{B}}_k$ and $\boldsymbol{C}_k$, for $k = 1,\ 2,\ 3$	33
Figure 3.11	A pair of coplanar triangles $\boldsymbol{ABCD}$	37
Figure 3.12	The ratio $\alpha : \beta$	38
Figure 3.13	Effect of γ to a pair of triangles (fixed $\alpha : \beta$)	39
Figure 3.14	Repositioning the point $\boldsymbol{C}$	41
Figure 3.15	Repositioning the points $\boldsymbol{A}$ and $\boldsymbol{D}$ with fixed ratio $\alpha : \beta$	42

Figure 4.1	Three different positions of point $\boldsymbol{V}$	44
Figure 4.2	Function $G(s)$ for $s > 0$	49
Figure 4.3	A pair of triangles	51
Figure 5.1	Triangle T	55
Figure 5.2	Control points of a triangular Bézier patch $\boldsymbol{P}$	57
Figure 5.3(a)	Control points of cubic Bézier boundary curves	59
Figure 5.3(b)	Boundary control points of quartic Bézier triangular patch	59
Figure 5.4(a)	Triangles on tangent plane at vertex $\boldsymbol{O}$	60
Figure 5.4(b)	An overlap between the tangent triangles	60
Figure 5.5	Modification of a Bézier point next to vertex $\boldsymbol{O}$	63
Figure 5.6	Range of γ_0	67
Figure 5.7	Control points for two adjoining Bézier patches with $\boldsymbol{b}_{0,4-k,k} = \boldsymbol{c}_{0,4-k,k}$, $k = 0, 1, \ldots, 4$	69
Figure 5.8	G^1 continuity of constant $\alpha(t)$ and $\beta(t)$	72
Figure 5.9	G^1 continuity of linear $\alpha(t)$, $\beta(t)$ and $\gamma(t)$	73
Figure 5.10	Modification of a couple of inner Bézier points	76
Figure 6.1	The linear interpolant to data of Example 1	80
Figure 6.2(a)	The unconstrained surface of Example 1 and the constraint plane	80
Figure 6.2(b)	The unconstrained surface of Example 1 (a side view)	80
Figure 6.3(a)	The range restricted surface of Example 1 and the constraint plane	81
Figure 6.3(b)	The range restricted surface of Example 1 (a side view)	81
Figure 6.4(a)	Pairs of tangent triangles at the shared vertices of unconstrained surface and the lower bound plane	81
Figure 6.4(b)	Pairs of tangent triangles at the shared vertices of range restricted surface and the lower bound plane	81

Figure 6.5	The linear interpolant of Example 2 and the constraint plane	82
Figure 6.6(a)	The unconstrained surface of Example 2 and the constraint plane	82
Figure 6.6(b)	The unconstrained surface of Example 2 (a side view)	82
Figure 6.7(a)	The range restricted surface of Example 2 and the constraint plane	83
Figure 6.7(b)	The range restricted surface of Example 2 (a side view)	83
Figure 6.8	The triangular mesh of Example 3	85
Figure 6.9(a)	The unconstrained surface of Example 3 and the constraint plane	85
Figure 6.9(b)	The unconstrained surface of Example 3 (a side view)	85
Figure 6.10(a)	The range restricted surface of Example 3 and the constraint plane	86
Figure 6.10(b)	The range restricted surface of Example 3 (a side view)	86
Figure 6.11	The triangular mesh of Example 4	88
Figure 6.12(a)	The unconstrained surface of Example 4 and the constraint plane	88
Figure 6.12(b)	The unconstrained surface of Example 4 (a side view)	88
Figure 6.13(a)	The range restricted surface of Example 4 and the constraint plane	89
Figure 6.13(b)	The range restricted surface of Example 4 (a side view)	89
Figure 6.14	The triangular mesh of Example 5	91
Figure 6.15(a)	The unconstrained surface of Example 5 and the constraint plane	91
Figure 6.15(b)	The unconstrained surface of Example 5 (a side view)	91
Figure 6.16(a)	The range restricted surface of Example 5 and the constraint plane	92
Figure 6.16(b)	The range restricted surface of Example 5 (a side view)	92

Figure 6.17	The linear interpolant of Example 6	93
Figure 6.18	The unconstrained surface of Example 6	93
Figure 6.19(a)	The range restricted surface of Example 6	94
Figure 6.19(b)	The range restricted surface of Example 6 and the constraint plane $z = 1$ (a side view)	94
Figure A(a)		100
Figure A(b)		100

INTERPOLASI DATA G^1 JULAT TERHAD DENGAN TAMPALAN SEGI TIGA BÉZIER

ABSTRAK

Pembinaan permukaan berparameter G^1 julat terhad kepada data yang semua terletak di sebelah satu satah kekangan dipertimbangkan. Permukaan interpolasi dibina secara cebis demi cebis daripada gabungan cembung tiga tampalan segi tiga Bézier kuartik. Syarat cukup untuk keselanjaran satah tangen sepanjang sempadan dua tampalan Bézier kuartik dibentangkan. Syarat cukup penghadan julat diterbitkan di mana batas bawah dikenakan kepada titik-titik Bézier. Di samping itu, syarat tambahan untuk memastikan penghadan julat dua tampalan segi tiga Bézier bersebelahan dibentangkan. Vektor normal dianggarkan pada tapak data dengan satu kaedah penganggaran setempat. Titik Bézier pada mulanya ditentukan dengan titik data dan vektor normal anggaran pada data supaya interpolan adalah berkeselanjaran G^1 pada salah satu sempadan segi tiga. Titik Bézier kemudian diubah jika perlu supaya syarat cukup penghadan julat dipenuhi bersama syarat keselanjaran. Permukaan terhasil adalah berkeselanjaran G^1 dan terletak di sebelah satah kekangan yang sama seperti data yang diberikan. Beberapa contoh dipersembahkan secara grafik.

G^1 RANGE RESTRICTED DATA INTERPOLATION USING BÉZIER TRIANGULAR PATCH

ABSTRACT

The construction of range restricted G^1 parametric surface to data that all lie on one side of a constraint plane is considered. The interpolating surface is developed piecewise as the convex combination of three quartic Bézier triangular patches. Sufficient tangent plane continuity conditions along the common boundary of two adjacent quartic Bézier triangular patches are presented. Sufficient range restriction conditions are derived which imposed the lower bound to Bézier points. In addition, supplementary conditions to ensure the range restriction of two adjoining triangular Bézier patches are presented. The normal vectors are estimated at the data sites by a local estimation method. The Bézier points are initially determined by the data points and the estimated normal vectors at data, and such that the interpolant is G^1 continuous across one of the triangle boundaries. The Bézier points are then modified if necessary so that the sufficient range restriction condition is fulfilled in conjunction with the continuity condition. The resulting surface is G^1 continuous and lies on the same side of the constraint plane as the given data. Some examples are presented graphically.

CHAPTER 1

INTRODUCTION

Computer Aided Geometric Design (CAGD) is a branch of applied mathematics concerned with the representation, approximation and computation of free-form curves, surfaces and volumes by using computer technology. It has a wide variety of applications in the manufacturing of products such as the design of planes and ships, in the representation of physical phenomena such as geophysical maps, and in numerous other situations.

A common problem in scientific visualization is to present the three-dimensional data as a surface or a contour map. Scientific visualization provides a means of understanding various physical phenomena, from limited or incomplete information. The data that are known represent only a sample and may not be sufficient to let one visualize the entire entity. As such one uses interpolation to construct an empirical model which matches the data samples and approximates the unknown entity at intermediate locations. There are some properties inherent in the data like convexity, monotonicity (for non-parametric data) and positivity which one wishes to preserve. It is the last of these that is of interest in this thesis, namely if all the sampled data are positive, then the interpolant should be positive everywhere.

Positivity preserving is particularly important when visualizing a physical entity that should not possibly be negative. For example, if the data represent a material

concentration or pressure, a probability density, or the progress of an irreversible process, negative values of an interpolant are not physically meaningful. Examples of studies in the area of positivity-preservation for surface can be found in (Brodlie *et al*., 1995) described the problem of interpolation subject to simple linear constraints. It looks at the problem of constructing a function $u(x,y)$ of two variables from data on a rectangular mesh, such that $u(x,y)$ is non-negative. Sufficient conditions are derived to ensure a positive piecewise bicubic interpolant results from positive data. The problem of non-negativity is then generalized to range restricted interpolation such that $u(x,y)$ is greater or smaller than some linear functions.

Although the necessary and sufficient non-negativity conditions for bivariate quadratic polynomials have been established (Nadler, 1992), the necessary and sufficient non-negativity conditions for bivariate polynomials of higher degree are not derived yet. Sufficient non-negativity conditions for cubic and quartic polynomials were given in (Chan & Ong, 2001), (Piah *et al*., 2005) and (Schumaker & Speleers, 2010). Here, we should note that sufficient condition means the statement is truth to its consequent, while necessary and sufficient condition means the former statement is true if and only if the latter is true.

The problem of range restricted interpolation to irregularly spaced data is addressed in which the parametrically defined interpolant is restricted to lie within a specific region. This problem occurs in many practical situations where bounded data are gathered experimentally or via simulation studies. There are many approaches to scattered data interpolation, a good review is given in (Lodha & Franke, 2000).

The common approach to this problem is based on a triangulation of given data, followed by a piecewise construction of the interpolant - one piece per triangle. A simple technique of this type is piecewise linear interpolation. Obviously, the resulting interpolant remains within the bounds of the data. However, it is only C^0 continuous. The smoothness remains an important issue in the problem. Smoother interpolant can be obtained by deeply refining the triangular mesh of given data. Many attempts have been made to produce a smooth non-negative interpolant such as in (Herrmann *et al*., 1996), (Ong & Wong, 1996), (Chan & Ong, 2001), (Piah *et al*., 2005), (Piah *et al*., 2006) and (Cheng *et al*., 2009).

Herrmann *et al*. (1996) have constructed a range restricted bivariate C^1 interpolant using quadratic splines on a Powell–Sabin refinement of a triangulation of scattered data subject to piecewise quadratic lower and upper bounds. The sufficient range restriction conditions are derived in the form of a solvable system of linear inequalities with the gradients as parameters.

Goodman *et al*. (1995) proposed a method of estimating gradients at scattered data points. It requires significantly less computation and produces comparable accuracy to the existing least-squares minimization method. The method was used to construct a smooth C^1 surface for the scattered data interpolation.

Ong & Wong (1996) have derived a local C^1 scattered data interpolation scheme subject to constant lower and upper bounds. The side vertex method is applied for interpolation in triangles and rational cubics are used for univariate interpolation along the line segments joining a vertex to the opposite edge of a

triangle.

Chan & Ong (2001) and Piah *et al*. (2005) described a local C^1 range restricted scattered data interpolation scheme. The interpolating surface is obtained piecewise as the convex combination of three cubic Bézier triangular patches. Lower bound on the Bézier ordinates is derived to ensure that the non-negativity of a cubic Bézier triangular patch. Indeed Piah *et al*. (2005) proposed a more relaxed lower bound. The gradient at each data site is modified subject to the non-negativity conditions.

Piah *et al*. (2006) and Cheng *et al*. (2009) generated non-parametric surfaces that interpolate positive scattered data. The surfaces comprise piecewise quartic Bézier triangles. The schemes are very similar to that of cubic interpolation scheme. Sufficient non-negativity conditions on quartic Bézier ordinates are derived. The gradient at each data site are used to modify Bézier ordinates if necessary.

All the range restricted surfaces cited above are non-parametric. For the time being, no scheme was presented on the problem of range restricted data interpolation with geometric G^1 continuity except in (Piah *et al*., 2006) which described the generation of surfaces that interpolate positive scattered data with the simplest G^1 continuity conditions. Free-form surface design is typically accomplished in a piecewise manner. It is preferable that the composite surface not to be viewed as a map of a triangulated domain on $\mathbb{R}^2$ into $\mathbb{R}^3$. Therefore, the composite surface shall be considered as many maps of one domain triangle onto different patches of the surface (Piper, 1987). The G^1 continuity is independent of the parameterization

of the surfaces. For parametric case, quartics are the lowest degree triangular Bézier patches that are suitable for the construction of a composite G^1 surface.

Motivated by previous work, in this thesis the problem of range restricted data interpolation is considered where the surface is defined parametrically by quartic Bézier triangular patches subject to a given constraint plane. This extends the existing works from the parametric C^1 continuity to geometric G^1 continuity and non-parametric interpolation to parametric interpolation. The resulting surface interpolant is piecewise a convex combination of three quartic Bézier triangular patches interpolating the prescribed data. The sufficient G^1 continuity condition along the common boundary of two adjacent quartic Bézier triangular patches is presented. This condition can be simplified to the C^1 continuity condition when certain conditions are met. The Bézier points of quaritc Bézier triangular patch are determined by the given data points and normal vectors at data sites, and such that ensures G^1 continuity across one of the triangle boundaries. The Bézier points as obtained which do not satisfy the lower bound of range restriction condition shall be adjusted to ensure the surface to be range restricted. In addition, supplementary conditions of range restriction are derived to ensure two adjacent Bézier patches which join smoothly are range restricted. These conditions have not been alerted in earlier work.

The outline of the thesis is as follows. In Chapter 2, the triangular Bézier surface is introduced in terms of generalized Bernstein polynomials. Barycentric coordinates are used to deal with triangular domain of Bézier surface. Some useful

properties of Bézier triangle are given. Degree elevation of Bézier curve is given to raise the degree of a Bézier curve without changing the shape of the curve. Directional derivatives of Bézier triangle are described. A method of estimating unit surface normal vector at given data site is proposed.

In Chapter 3, the sufficient G^1 continuity conditions along the common boundary of two adjacent triangular Bézier patches are derived. The coefficients in the tangent plane continuity conditions are prescribed to be linear functions. The structure of G^1 continuity is illustrated geometrically and its properties are remarked. The C^1 continuity condition is also presented in this chapter.

In Chapter 4, the sufficient range restriction condition is introduced for a parametric quartic Bézier triangular patch to lie on the same side of a given constraint plane as data points. A lower bound on the Bézier points is derived to ensure range restriction for a quartic Bézier triangular patch. When the concerned constraint plane is the xy-plane, the condition is simplified to as the sufficient non-negativity condition given in (Piah *et al*., 2006). Supplementary conditions to be satisfied are given in order to guarantee the range restriction for two adjoining quartic Bézier patches. An example is also given to show that the lack of supplementary conditions may cause two adjacent Bézier patches failed to satisfy the lower bounds of range restriction condition in conjunction with the continuity condition.

In Chapter 5, a local scheme for parametric G^1 range restricted scattered data interpolation is presented. The scheme fit a composite surface to scattered data points

that all lie one side of a constraint plane. Each surface patch is constructed as the convex combination of three quartic Bézier triangular patches. The continuity condition and the range restriction condition presented in Chapters 3 and 4 are imposed to Bézier points in order to obtain a range restricted G^1 interpolant. Lastly, some graphical examples, the conclusion and suggestions for the future work are given in Chapter 6.

CHAPTER 2

TRIANGULAR BERNSTEIN-BÉZIER PATCH

2.0 Introduction

Triangular Bézier patch in terms of Bernstein polynomials have been widely implemented in Computer Aided Geometric Design as a basic model for generating free-form surface. Such popularity is certainly due to its powerful geometric properties and to its simplicity of manipulation. Barycentric coordinate is used as coordinate system to deal with the triangular domain of Bézier patch.

In this chapter, the definition of triangular Bézier patch and some of its useful properties are expressed. Directional derivatives are considered upon Bézier patch. Besides, degree elevation of Bézier curve is discussed to raise the degree of a Bézier curve without modifying the shape of the curve. This will be used in Chapter 5 on elevating cubic boundary curves of a Bézier patch to quartics. Lastly a method for estimating normal vectors at vertices of a triangle is presented. The estimated normal vectors are utilized to construct boundary curves of a Bézier patch.

2.1 Bernstein Polynomials

There are two forms (univariate and bivariate) of Bernstein basis for the space of polynomials (Hoschek & Lasser, 1993). The univariate Bernstein polynomials of degree n are defined as

$$B_i^n(t) = \binom{n}{i} t^i (1-t)^{n-i}, \qquad i = 0, 1, \ldots, n, \qquad 0 \le t \le 1 \qquad (2.1)$$

where the binomial coefficients are given by

$$\binom{n}{i} = \frac{n!}{i!(n-i)!}.$$

Obviously, there are $(n+1)$ Bernstein polynomials of degree n. These polynomials are quite easy to be formulated as the binomial coefficients can be obtained via Pascal's triangle. They have a number of useful properties. One of them is that all the Bernstein polynomials are non-negative over the parametric interval [0, 1] i.e.,

$$B_i^n(t) \ge 0.$$

Other is that the Bernstein polynomials form a partition of unity (Farin, 1996)

$$\sum_{i=0}^{n} B_i^n(t) = 1$$

and the product of an m^{th} degree Bernstein polynomial with an n^{th} degree Bernstein polynomial is $(m+n)^{\text{th}}$ Bernstein polynomial

$$B_i^m(t) B_j^n(t) = \frac{\binom{m}{i}\binom{n}{j}}{\binom{m+n}{i+j}} B_{i+j}^{m+n}(t) \quad .$$

The bivariate Bernstein polynomials are commonly presented in the form of

barycentric coordinate. Barycentric coordinate is used as ideal coordinate system when dealing with a triangle. Consider a triangle T with vertices $\boldsymbol{V}_1$, $\boldsymbol{V}_2$ and $\boldsymbol{V}_3$ as in Figure 2.1, any point $\boldsymbol{V}$ on the triangle can be written as a barycentric combination of $\boldsymbol{V}_3$, $\boldsymbol{V}_1$, $\boldsymbol{V}_2$ as

$$\boldsymbol{V} = u\boldsymbol{V}_3 + v\boldsymbol{V}_1 + w\boldsymbol{V}_2$$

where $u,\ v,\ w \geq 0$ and $u+v+w=1$.

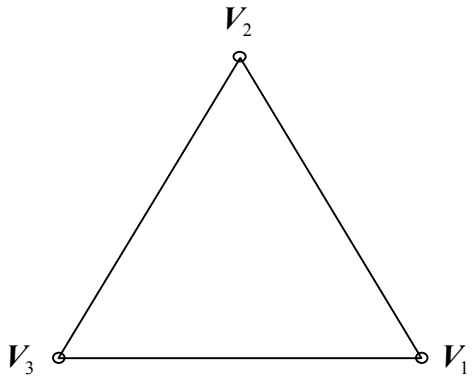

Figure 2.1 Triangle T with vertices $\boldsymbol{V}_1$, $\boldsymbol{V}_2$, $\boldsymbol{V}_3$

Due to univariate Bernstein polynomials are the terms of the binomial expansion of $\left[t+(1-t)\right]^n$, therefore the bivariate Bernstein polynomials are defined by

$$B_{i,j,k}^{n}(u,v,w) = \frac{n!}{i!\,j!\,k!}u^i v^j w^k, \tag{2.2}$$

where $u,\ v,\ w \geq 0$, $u+v+w=1$, and integers $i,\ j,\ k \geq 0$, $i+j+k=n$. Although $B_{i,j,k}^{n}(u,v,w)$ looks trivariate, it is not, since $u+v+w=1$. The bivariate Bernstein polynomials possess the properties that

$$B_{i,j,k}^{n}(u,v,w) \geq 0 \ ,$$

and

$$\sum_{\substack{i+j+k=n \\ i,j,k\geq 0}} B_{i,j,k}^{n}(u,v,w)=1 \quad .$$

2.2 Bézier Curve

Bézier curve is a parametric curve widely used in geometric modelling. Given $(n+1)$ control points $\boldsymbol{b}_0, \boldsymbol{b}_1, \ldots, \boldsymbol{b}_n \in \mathbb{R}^3$, a Bézier curve is defined explicitly by (Farin, 1996)

$$\boldsymbol{P}(t)=\sum_{i=0}^{n} \boldsymbol{b}_i B_i^n(t), \qquad 0\leq t\leq 1 \tag{2.3}$$

where $B_i^n(t)$ are Bernstein polynomials in (2.1). The polygon formed by connecting control points $\boldsymbol{b}_0, \boldsymbol{b}_1, \ldots, \boldsymbol{b}_n$ is called Bézier polygon or control polygon of Bézier curve. The derivative vector to Bézier curve $\boldsymbol{P}(t)$ is another Bézier polynomial

$$\boldsymbol{P}'(t)=\sum_{i=0}^{n-1} \bar{\boldsymbol{b}}_i B_i^{n-1}(t) \tag{2.4}$$

where coefficients

$$\bar{\boldsymbol{b}}_i=\boldsymbol{b}_{i+1}-\boldsymbol{b}_i, \qquad i=0, 1, \ldots, n-1.$$

2.3 Degree Elevation of Bézier Curve

Degree elevation is an algorithm that raises the degree of Bézier curve from n to $(n+1)$ and adds a control point as well without changing the shape of the curve. The process of degree elevation may be repeated. As every polynomial curve of degree n can be expressed as a polynomial curve of degree $(n+1)$, hence for a Bézier curve of degree n with control points $\boldsymbol{b}_0, \boldsymbol{b}_1, \ldots, \boldsymbol{b}_n$, the curve

$$\boldsymbol{P}(t) = \sum_{i=0}^{n} \boldsymbol{b}_i B_i^n(t), \qquad 0 \le t \le 1$$

$$= \sum_{i=0}^{n+1} \boldsymbol{b}_i^* B_i^{n+1}(t)$$

where control points $\boldsymbol{b}_0^*, \boldsymbol{b}_1^*, \ldots, \boldsymbol{b}_{n+1}^*$ are given as (Farin, 1996)

$$\boldsymbol{b}_i^* = \frac{i}{n+1}\boldsymbol{b}_{i-1} + \left(1 - \frac{i}{n+1}\right)\boldsymbol{b}_i, \qquad i = 0, 1, \ldots, n+1. \tag{2.5}$$

2.4 Triangular Bézier Patch

In this section, a triangular Bézier patch is presented using the bivariate Bernsterin polynomials in (2.2). For easier understanding, the concept of a triangular patch is described first. A triangular patch is a mapping $\boldsymbol{S}: T \to \mathbb{R}^3$ where parameter set $T \subset \mathbb{R}^2$ is a triangle described by barycentric coordinates of (u, v, w). Triangular Bézier patch is a surface defined over the domain triangle T. The patch is based on control points $\boldsymbol{b}_{i,j,k}$ arranged in space and are assigned three indexes i, j, k, such that $i, j, k \ge 0$ and $i + j + k = n$. When at least one of indexes turn to zero, $\boldsymbol{b}_{i,j,k}$ is referred to a boundary control point, otherwise it is referred to as an inner control point. The value of n is selected by the user depending on how large and complex the patch should be and how many points are given. The triangular Bézier patch $\boldsymbol{P}$ of degree n on domain T is defined parametrically as (Farin, 1986)

$$\boldsymbol{P}(u,v,w) = \sum_{\substack{i+j+k=n \\ i,j,k \ge 0}} \boldsymbol{b}_{i,j,k} B_{i,j,k}^n(u,v,w), \tag{2.6}$$

where $u, v, w \ge 0$, $u + v + w = 1$ and $B_{i,j,k}^n(u,v,w)$ are the Bernstein polynomials

defined by (2.2). In particular, the quartic Bézier patch ($n = 4$) is

$$\begin{aligned}\boldsymbol{P}(u,v,w) = {} & u^4\boldsymbol{b}_{4,0,0} + 4u^3v\boldsymbol{b}_{3,1,0} + 4u^3w\boldsymbol{b}_{3,0,1} + 6u^2v^2\boldsymbol{b}_{2,2,0} + 12u^2vw\boldsymbol{b}_{2,1,1} + \\ & 6u^2w^2\boldsymbol{b}_{2,0,2} + 4uv^3\boldsymbol{b}_{1,3,0} + 12uv^2w\boldsymbol{b}_{1,2,1} + 12uvw^2\boldsymbol{b}_{1,1,2} + 4uw^3\boldsymbol{b}_{1,0,3} + \\ & v^4\boldsymbol{b}_{0,4,0} + 4v^3w\boldsymbol{b}_{0,3,1} + 6v^2w^2\boldsymbol{b}_{0,2,2} + 4vw^3\boldsymbol{b}_{0,1,3} + w^4\boldsymbol{b}_{0,0,4}\,.\end{aligned}$$

The coefficients in (2.6) are vector-valued in $\mathbb{R}^3$ as

$$\boldsymbol{b}_{i,j,k} = \left(x_{i,j,k},\ y_{i,j,k},\ z_{i,j,k} \right).$$

They can be real numbers in $\mathbb{R}$ by considering $z_{i,j,k}$ which are then referred to as Bézier ordinates and name non-parametric triangular Bézier patch. In the latter case, the Bézier patch is actually a scalar-valued function in which the Bézier ordinates are associated with the abscissas $\left(x_{i,j,k},\ y_{i,j,k} \right)$ that defined by the parameter values $\left(\frac{i}{n}, \frac{j}{n}, \frac{k}{n} \right)$ on T.

The three boundary curves of Bézier patch $\boldsymbol{P}$ are obtained from (2.6) by setting each of the three parameters to zero respectively. For example, the boundary curve along $u = 0$ (i.e., edge $\boldsymbol{V}_1\boldsymbol{V}_2$) is

$$\begin{aligned}\boldsymbol{P}(0,v,w) &= \sum_{\substack{i+j+k=n \\ i,j,k\geq 0}} \boldsymbol{b}_{i,j,k} B^n_{i,j,k}(0,v,w) \\ &= \sum_{\substack{j+k=n \\ j,k\geq 0}} \boldsymbol{b}_{0,j,k} B^n_{0,j,k}(0,v,w)\end{aligned}$$

where $v + w = 1$. Observe that boundary curve $\boldsymbol{P}(0,v,w)$ can be rewritten as

$$\boldsymbol{P}(v) = \sum_{j=0}^{n} \boldsymbol{b}_{0,j,n-j} B^n_j(v), \qquad 0 \leq v \leq 1$$

that is a Bézier curve of degree n with control points $\boldsymbol{b}_{0,j,n-j}$, $j = 0, 1, \ldots, n$. Obviously, boundary curve $\boldsymbol{P}(0,v,w)$ also can be rewritten as

$$\boldsymbol{P}(w)=\sum_{k=0}^{n}\boldsymbol{b}_{0,n-k,k}B_k^n(w),\qquad 0\le w\le 1.$$

The other two Bézier curves along the edges $v=0$ and $w=0$ can be obtained similarly.

Corner points can also be obtained from (2.6) when any two of the three barycentric parameters are set to zero. They can be expressed as

$$\boldsymbol{P}(1,0,0)=\boldsymbol{b}_{n,0,0},$$

$$\boldsymbol{P}(0,1,0)=\boldsymbol{b}_{0,n,0},$$

$$\boldsymbol{P}(0,0,1)=\boldsymbol{b}_{0,0,n}.$$

These imply that the corner Bézier points $\boldsymbol{b}_{n,0,0}$, $\boldsymbol{b}_{0,n,0}$, $\boldsymbol{b}_{0,0,n}$ lie on the surface at vertices $\boldsymbol{V}_3$, $\boldsymbol{V}_1$, $\boldsymbol{V}_2$ respectively.

2.5 Directional Derivatives of Bézier Patch

For a triangular Bézier patch, because of the barycentric parameterization, it is more ideal to use directional derivatives instead of partial derivatives. The directional derivative of a multivariate differentiable function along a given direction d at a given point $\boldsymbol{V}$ intuitively represents the instantaneous rate of change of the function, moving through that point in the given direction. It therefore generalizes the notion of partial derivative.

A direction at the parametric domain of a triangular Bézier patch is defined by two points in the domain. Let $\boldsymbol{A}=(u_0,\ v_0,\ w_0)$ and $\boldsymbol{B}=(u_1,\ v_1,\ w_1)$, where $u_0+v_0+w_0=1$ and $u_1+v_1+w_1=1$, be any two points in the domain triangle T.

Obviously, barycentric vector

$$\boldsymbol{B}-\boldsymbol{A}=\left(u_1-u_0,\ v_1-v_0,\ w_1-w_0\right)$$

has that sum of all its components is zero.

Consider a direction in parametric domain indicated by $d=\left(f,\ g,\ h\right)$, thus the directional derivative of Bézier surface $\boldsymbol{P}$ with respect to vector d is defined by

$$D_d\boldsymbol{P}\left(u,\ v,\ w\right)=f\,\boldsymbol{P}_u\left(u,\ v,\ w\right)+g\,\boldsymbol{P}_v\left(u,\ v,\ w\right)+h\,\boldsymbol{P}_w\left(u,\ v,\ w\right) \tag{2.7}$$

where $\boldsymbol{P}_u$, $\boldsymbol{P}_v$, $\boldsymbol{P}_w$ indicate the partial derivatives of $\boldsymbol{P}$ with respect to u, v and w respectively. The partial derivative of $\boldsymbol{P}$ with respect to u is

$$\begin{aligned}\boldsymbol{P}_u\left(u,v,w\right) &=\frac{\partial}{\partial u}\boldsymbol{P}\left(u,v,w\right)\\ &=n\sum_{\substack{i+j+k=n\\ i,j,k\geq 0}}\frac{\left(n-1\right)!}{\left(i-1\right)!\,j!\,k!}u^{i-1}v^j w^k\boldsymbol{b}_{i,j,k}\\ &=n\sum_{\substack{i+j+k=n-1\\ i,j,k\geq 0}}\frac{\left(n-1\right)!}{i!\,j!\,k!}u^i v^j w^k\boldsymbol{b}_{i+1,j,k}\\ &=n\sum_{\substack{i+j+k=n-1\\ i,j,k\geq 0}}\boldsymbol{b}_{i+1,j,k}B_{i,j,k}^{n-1}\left(u,v,w\right).\end{aligned}$$

Owing to symmetry, the other two partial derivatives can be formulated in the same way as

$$\boldsymbol{P}_v\left(u,v,w\right)=n\sum_{\substack{i+j+k=n-1\\ i,j,k\geq 0}}\boldsymbol{b}_{i,j+1,k}B_{i,j,k}^{n-1}\left(u,v,w\right),$$

$$\boldsymbol{P}_w\left(u,v,w\right)=n\sum_{\substack{i+j+k=n-1\\ i,j,k\geq 0}}\boldsymbol{b}_{i,j,k+1}B_{i,j,k}^{n-1}\left(u,v,w\right).$$

Substituting these partial derivatives into (2.7), it leads to (Farin, 1986)

$$D_d\boldsymbol{P}\left(u,\ v,\ w\right)=n\sum_{\substack{i+j+k=n-1\\ i,j,k\geq 0}}\left(f\boldsymbol{b}_{i+1,j,k}+g\,\boldsymbol{b}_{i,j+1,k}+h\,\boldsymbol{b}_{i,j,k+1}\right)B_{i,j,k}^{n-1}\left(u,v,w\right). \tag{2.8}$$

Next, a boundary point is considered. Let $e_1=\left(0,\ v,\ 1-v\right)$, $0\leq v\leq 1$, be a

point on the edge $\boldsymbol{V}_1\boldsymbol{V}_2$, see Figure 2.2. Consider a barycentric direction along the edge $\boldsymbol{V}_1\boldsymbol{V}_2$, let $d=(0,\,-1,\,1)$. From (2.8), the directional derivative of $\boldsymbol{P}$ at point e_1 is given by

$$D_{(0,-1,1)}\boldsymbol{P}(e_1)=n\sum_{k=0}^{n-1}\left(\boldsymbol{b}_{0,n-1-k,k+1}-\boldsymbol{b}_{0,n-k,k}\right)B_k^{n-1}(e_1).$$

It is clear that the directional derivative along the edge $\boldsymbol{V}_1\boldsymbol{V}_2$ is determined completely by the control points of that boundary.

Suppose a direction across the edge is concerned, let $d=(1,\,-0.5,\,-0.5)$. From (2.8), the directional derivative of $\boldsymbol{P}$ at point e_1 along direction $(1,\,-0.5,\,-0.5)$ is

$$D_{(1,-0.5,-0.5)}\boldsymbol{P}(e_1)=n\sum_{k=0}^{n-1}\left(\boldsymbol{b}_{1,n-1-k,k}-\frac{1}{2}\boldsymbol{b}_{0,n-k,k}-\frac{1}{2}\boldsymbol{b}_{0,n-1-k,k+1}\right)B_k^{n-1}(e_1).$$

Obviously, the cross-boundary derivatives are determined by the control points of the boundary and those of the next row to the boundary.

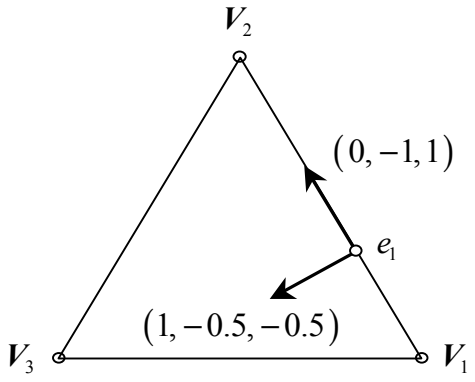

Figure 2.2 Directions at a boundary point e_1

From the description given above, for the boundary curve defined along an edge connecting two vertices, the corner Bézier point and the Bézier point next to it determine the tangent to the boundary at the endpoint. Furthermore, the corner

Bézier point and its two neighboring Bézier points determine the tangent plane to the surface at the corner.

2.6 Normal Estimation

In this section a method for estimating normal vector at given data set is proposed. The estimated normal vectors are used to generate curve network of interpolating surface which will be discussed precisely in Chapter 5. Suppose a set of triangulated 3D data is given. A unit vector which will act as surface normal vector is estimated at each data point by using convex combination of the normal vectors to the neighboring triangles of which the point is a vertex. The weight in convex combination is determined by the size of concerned triangle. This estimation method is motivated by the method of estimating derivatives at data point introduced in (Goodman *et al*., 1995).

Consider a (inner) vertex $\boldsymbol{O}$ of a triangulated data and let π_i, $i = 1, 2, \ldots, m$, be the triangles which have $\boldsymbol{O}$ as a vertex as shown in Figure 2.3 (where $m = 6$). Denote $\boldsymbol{n}_i$, $i = 1, 2, \ldots, m$, as the unit normal vector to the triangle π_i. In order to obtain a precise approximant, $\boldsymbol{n}_i$ of surrounding triangles are defined with a fixed orientation such as

$$\boldsymbol{n}_i = \frac{\boldsymbol{OA}_i \times \boldsymbol{OA}_{i+1}}{\left\| \boldsymbol{OA}_i \times \boldsymbol{OA}_{i+1} \right\|}, \qquad \text{for } i = 1, 2, \ldots, m-1$$

and

$$\boldsymbol{n}_m = \frac{\boldsymbol{OA}_m \times \boldsymbol{OA}_1}{\left\| \boldsymbol{OA}_m \times \boldsymbol{OA}_1 \right\|}$$

where '×' indicates cross product of two vectors and $\|\boldsymbol{v}\|$ be the magnitude of a vector $\boldsymbol{v}$.

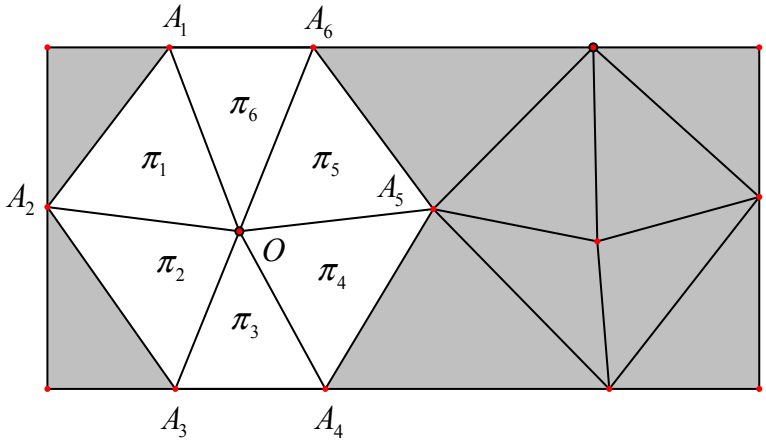

Figure 2.3 Vertex $\boldsymbol{O}$ and surrounding triangles

The normal vector at vertex $\boldsymbol{O}$ can be estimated by a convex combination of the unit normal vectors $\boldsymbol{n}_i$ of the surrounding triangles π_i expressed as

$$\boldsymbol{n}_O = \frac{\sum_{i=1}^{m} \lambda_i \boldsymbol{n}_i}{\sum_{i=1}^{m} \lambda_i}$$

where $\lambda_i = 1/\Delta_i$, $i = 1, 2, \ldots, m$, with Δ_i denotes the area of triangle π_i.

In above the vertex $\boldsymbol{O}$ is assumed in the interior of triangulated data. Special consideration should be taken when vertex $\boldsymbol{O}$ is on the boundary of the triangulation as in Figure 2.4. Denote π_i^*, $i = 1, \ldots, m$, as the triangle which shares the edge of π_i not containing $\boldsymbol{O}$. Denote also Δ_i^* as the area of triangle π_i^* and $\boldsymbol{n}_i^*$ as the unit normal vector to π_i^* defined as

$$\boldsymbol{n}_i^* = \frac{\boldsymbol{A}_i\boldsymbol{O}_i \times \boldsymbol{A}_i\boldsymbol{A}_{i+1}}{\left\| \boldsymbol{A}_i\boldsymbol{O}_i \times \boldsymbol{A}_i\boldsymbol{A}_{i+1} \right\|}, \qquad \text{for } i = 1, 2, \ldots, m.$$

If a triangle π_i meets at $\boldsymbol{O}$ but does not has adjacent triangle π_i^*, set $\Delta_i^* = 0$ and $\boldsymbol{n}_i^* = \boldsymbol{n}_i$. The normal vector at vertex $\boldsymbol{O}$ is now determined by

$$\boldsymbol{n}_O = \frac{\sum_{i=1}^{m} \frac{1}{\Delta_i} \frac{\left(2\Delta_i + \Delta_i^*\right)\boldsymbol{n}_i - \Delta_i \boldsymbol{n}_i^*}{\Delta_i + \Delta_i^*}}{\sum_{i=1}^{m} \frac{1}{\Delta_i}}.$$

The formulation of these normal vectors is not shown here, however it can be done by using simple Calculus and it is similar to that given in (Goodman *et al*., 1995). At last, unit normal vector at a data point $\boldsymbol{O}$ is defined by

$$\boldsymbol{N}_O = \frac{\boldsymbol{n}_O}{\|\boldsymbol{n}_O\|}.$$

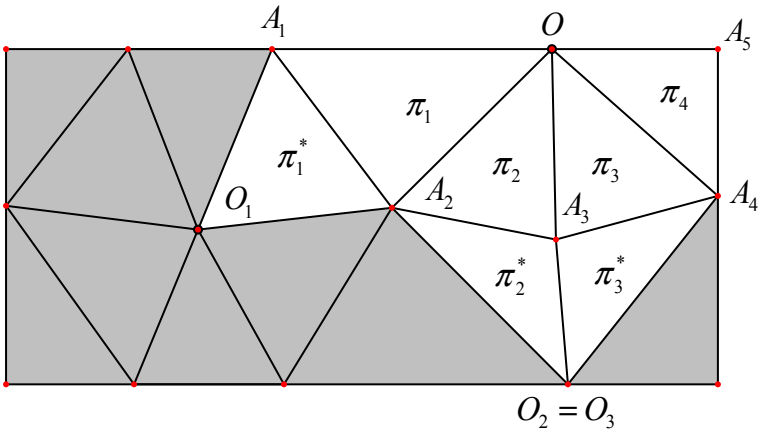

Figure 2.4 A boundary vertex $\boldsymbol{O}$

CHAPTER 3

G^1 CONTINUOUS JOIN OF QUARTIC BÉZIER TRIANGULAR PATCHES

3.1 C^1 Parametric Continuity Conditions

Consider two quartic Bézier triangular patches that are maps of two adjacent domain triangles, whose common edge is mapped onto the common boundary curve of the Bézier patches. Let $\boldsymbol{V}_1\boldsymbol{V}_2\boldsymbol{V}_3$ and $\boldsymbol{W}_1\boldsymbol{W}_2\boldsymbol{W}_3$ be two adjacent domain triangles with $\boldsymbol{V}_1 = \boldsymbol{W}_1$ and $\boldsymbol{V}_2 = \boldsymbol{W}_2$, see Figure 3.1. Barycentric coordinates (u, v, w) and (r, s, t) are used upon these two triangles respectively.

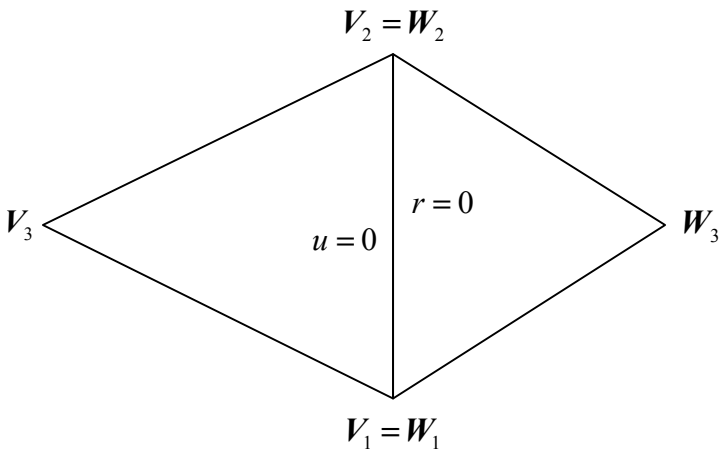

Figure 3.1 Two adjoining domain triangles

Suppose that the quartic Bézier triangular patches $\boldsymbol{S}_1(u, v, w)$ and $\boldsymbol{S}_2(r, s, t)$ on these two triangles have Bézier points $\boldsymbol{b}_{i,j,k}$ and $\boldsymbol{c}_{i,j,k}$ respectively, see figure below.

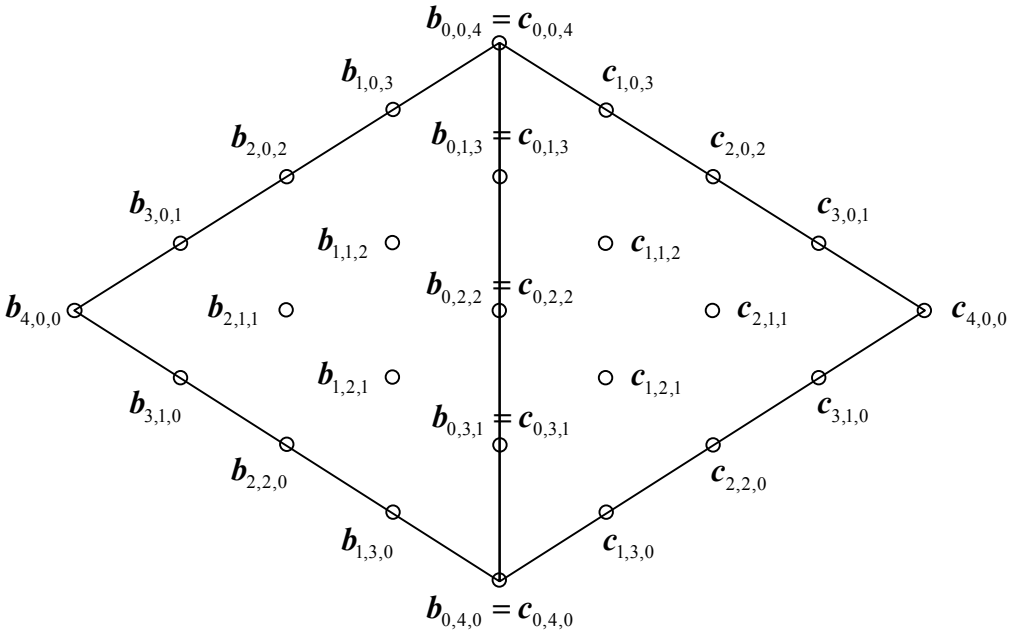

Figure 3.2 Control points of two adjacent quartic Bézier patches

A necessary and sufficient condition for the C^1 continuity along the common boundary of two adjacent Bézier patches is described in (Farin, 1996). For two Bézier patches to meet C^1 continuously along the common edge $\boldsymbol{V}_1\boldsymbol{V}_2$ ($u = 0$ and $r = 0$) the patches are required to be

$$\boldsymbol{S}_1(0,\ v,\ w) = \boldsymbol{S}_2(0,\ s,\ t)$$

and

$$D_{d_1}\boldsymbol{S}_1(0,\ v,\ w) = D_{d_r}\boldsymbol{S}_2(0,\ s,\ t)$$

where d_1 and d_r are the barycentric forms of a directional vector with respect to triangles $\boldsymbol{V}_1\boldsymbol{V}_2\boldsymbol{V}_3$ and $\boldsymbol{W}_1\boldsymbol{W}_2\boldsymbol{W}_3$ respectively. These yield

$$\boldsymbol{c}_{1,0,3} = \bar{u}\,\boldsymbol{b}_{1,0,3} + \bar{v}\,\boldsymbol{b}_{0,1,3} + \bar{w}\boldsymbol{b}_{0,0,4},$$

$$\boldsymbol{c}_{1,1,2} = \bar{u}\,\boldsymbol{b}_{1,1,2} + \bar{v}\,\boldsymbol{b}_{0,2,2} + \bar{w}\boldsymbol{b}_{0,1,3},$$

$$\boldsymbol{c}_{1,2,1} = \bar{u}\,\boldsymbol{b}_{1,2,1} + \bar{v}\,\boldsymbol{b}_{0,3,1} + \bar{w}\,\boldsymbol{b}_{0,2,2},$$

$$\boldsymbol{c}_{1,3,0} = \bar{u}\,\boldsymbol{b}_{1,3,0} + \bar{v}\,\boldsymbol{b}_{0,4,0} + \bar{w}\,\boldsymbol{b}_{0,3,1}$$

where $(\bar{u},\ \bar{v},\ \bar{w})$ are the barycentric coordinates of $\boldsymbol{W}_3$ with respect to $\boldsymbol{V}_3$, $\boldsymbol{V}_1$ and $\boldsymbol{V}_2$, i.e.

$$\boldsymbol{W}_3 = \bar{u}\,\boldsymbol{V}_3 + \bar{v}\,\boldsymbol{V}_1 + \bar{w}\,\boldsymbol{V}_2.$$

From the geometrical view, the C^1 continuity would be fulfilled if the shared pairs of triangles along the common boundary as illustrated in Figure 3.3 be coplanar and be an affine map of the two domain triangles.

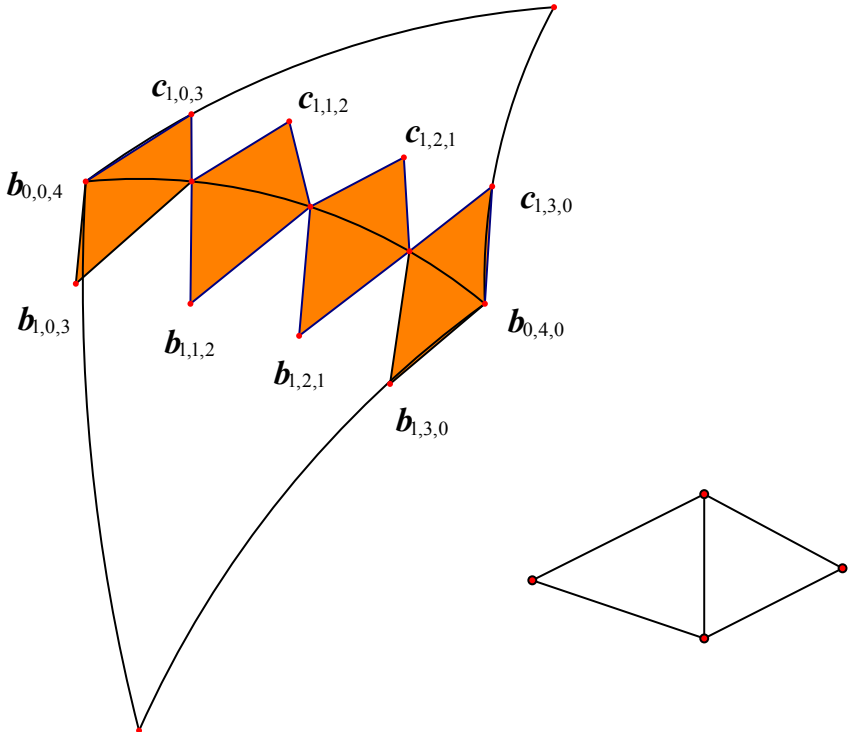

Figure 3.3 The shared pairs of triangles formed by control points of Bézier patches and the domain triangles

3.2 G^1 Geometric Continuity Conditions

The concept of G^1 continuity is that two patches with a common boundary

curve have a continuously varying tangent plane along that boundary curve (Farin, 1986). Geometric continuity is very useful in practice, in particular for modeling various kinds of spline surfaces where ordinary parametric continuity cannot be applied. More importantly, geometric continuity is invariant under parametric transformation, in contrast to parametric continuity. In this section mathematical description of geometric continuity G^1 between two quartic Bézier triangular patches $\boldsymbol{S}_1(u,v,w)$ and $\boldsymbol{S}_2(r,s,t)$ is presented in which the control points of the common boundary curve and the next "parallel" row in each patch are considered.

The quartic Bézier patches are G^0 continuous at a common boundary curve, provided that

$$\boldsymbol{S}_1(0,\ v,\ w) = \boldsymbol{S}_2(0,\ s,\ t)$$

with the parameterization $v = s$ and $w = t$ for every point on the common boundary curve. This can be ensured by $\boldsymbol{b}_{0,4,0} = \boldsymbol{c}_{0,4,0}$, $\boldsymbol{b}_{0,3,1} = \boldsymbol{c}_{0,3,1}$, $\boldsymbol{b}_{0,2,2} = \boldsymbol{c}_{0,2,2}$, $\boldsymbol{b}_{0,1,3} = \boldsymbol{c}_{0,1,3}$ and $\boldsymbol{b}_{0,0,4} = \boldsymbol{c}_{0,0,4}$.

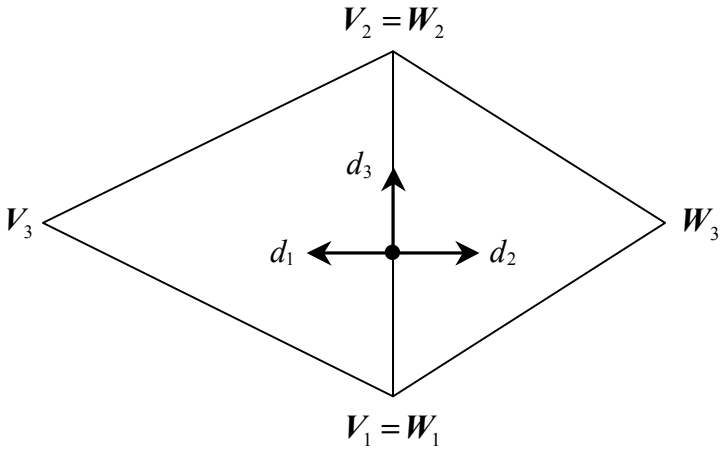

Figure 3.4 Three directions on domain triangles

Figure 3.4 shows three directions on the domain triangles. Let d_1 and d_2 be the barycentric directions across the common edge and generally they may in different directions. Vector d_3 indicates the direction along the common edge with $d_3 = (0, -1, 1)$. It follows immediately that

$$D_{d_3}\boldsymbol{S}_1(0, v, w) = D_{d_3}\boldsymbol{S}_2(0, s, t).$$

In order to obtain G^1 continuity every point on the common boundary curve must own a common tangent plane. This means derivaties $D_{d_1}\boldsymbol{S}_1$, $D_{d_2}\boldsymbol{S}_2$ and $D_{d_3}\boldsymbol{S}_1$ must lie on the same tangent plane. Therefore, the necessary and sufficient G^1 continuity condition is frequently presented in the form (Hoschek & Lasser, 1993)

$$\alpha(v,w)\,D_{d_1}\boldsymbol{S}_1(0,v,w) + \beta(s,t)\,D_{d_2}\boldsymbol{S}_2(0,s,t) + \gamma(v,w)\,D_{d_3}\boldsymbol{S}_1(0,v,w) = \boldsymbol{0}$$

where α, β and γ are functions of the parameters describing the common boundary curve with $\alpha\beta \neq 0$. The coplanarity condition above can be abbreviated as

$$\alpha(t)\,D_{d_1}\boldsymbol{S}_1(t) + \beta(t)\,D_{d_2}\boldsymbol{S}_2(t) + \gamma(t)\,D_{d_3}\boldsymbol{S}_1(t) = \boldsymbol{0} \tag{3.1}$$

for $0 \le t \le 1$. Note that the above condition allows variety of coefficient functions α, β and γ, but they are here restricted to be linear functions in t as

$$\begin{aligned}
\alpha(t) &= \alpha_0(1-t) + \alpha_1 t, \\
\beta(t) &= \beta_0(1-t) + \beta_1 t, \\
\gamma(t) &= \alpha_0(1-t) + \gamma_1 t
\end{aligned} \tag{3.2}$$

which may give variable values along the common boundary in particular at the two endpoints against constant coefficient functions. Thus more degree of freedom is gained compared to constant coefficients. As discussed in (Hoschek & Lasser, 1993), coefficients α, β and γ are advised not to have arbitrarily high degree. The